Diffusion of adatoms and small clusters on magnesium oxide surfaces



2009 J. Phys.: Condens. Matter 21 264001

(http://iopscience.iop.org/0953-8984/21/26/264001)

IOP PUBLISHING JOURNAL OF PHYSICS: CONDENSED MATTER

J. Phys.: Condens. Matter **21** (2009) 264001 (12pp) doi:10.1088/0953-8984/21/26/264001

# Diffusion of adatoms and small clusters on magnesium oxide surfaces

**Riccardo Ferrando**[1] **and Alessandro Fortunelli**[2]

[1] Dipartimento di Fisica, Università di Genova, Via Dodecaneso 33, I-16146 Genova, Italy
[2] IPCF/CNR, via G Moruzzi 1, I-56124 Pisa, Italy

E-mail: ferrando@fisica.unige.it and fortunelli@ipcf.cnr.it

Received 30 October 2008, in final form 14 November 2008
Published 11 June 2009
Online at stacks.iop.org/JPhysCM/21/264001

**Abstract**

The diffusion of isolated adatoms and small clusters is reviewed for transition and noble metals adsorbed on the (001) surface of magnesium oxide. While isolated adatoms diffuse by hopping among adsorption sites, small clusters such as dimers, trimers and tetramers already display a variety of diffusion mechanisms, from cluster hopping to rotation, sliding, leapfrog, walking, concertina, flipping, twisting, rolling and rocking. Since most of the available results are computational, the review is mostly related to theoretical work. Connection to experiments is discussed where possible, mostly by dealing with the consequences that adatom and small cluster mobility may have on the growth of larger aggregates on the MgO(001) surface.

(Some figures in this article are in colour only in the electronic version)

## 1. Introduction

The adsorption of metals on oxide surfaces has been extensively studied in recent years, especially in the context of the preparation of model nanocatalysts. Among oxide surfaces, the (001) surface of magnesium oxide has received a great deal of attention. Well-defined MgO(001) surfaces can be prepared with a low density of defects [1, 2].

The flat MgO(001) surface presents a perfect checkerboard of alternating oxygen and magnesium atoms. It is believed that most of the defects on this surface are oxygen vacancies ($F_s$ centers), double vacancies (in which a magnesium–oxygen dimer is missing) and steps. When adsorbed on a flat MgO(001) surface, metal atoms preferentially sit on top of oxygen atoms [3]. Defect sites can provide some extra binding [4, 5].

Metals on MgO(001) very often tend to form well-defined three-dimensional aggregates, because the interactions between metal atoms are usually stronger than the interactions between metal atoms and the substrate [1, 6]. The shape of the aggregates depends on a complex interplay between metal–metal and metal–oxide interactions [7–9]. Depending on the metal and on the size of the nanoparticle, fcc structures can be produced in different epitaxies with the substrate, such as cube-on-cube (001) [1, 10] and (111) epitaxy [2, 11], as in the cases of Ag, Au, Pd and Pt. If the mismatch between the bulk metal lattice spacing and the oxygen–oxygen distance is large, as in Ni/MgO(001), even hcp clusters can be produced [12, 9].

A key step for understanding how these aggregates form on the surface is the study of the diffusion of single atoms and small clusters. In fact, their mobility is crucial in determining whether nucleation occurs preferentially at defects or on the flat surface. Fast diffusion causes nucleation at defects only, whereas slow diffusion allows nucleation also on flat terraces.

At variance with metal-on-metal diffusion [13], we do not expect complicated diffusion mechanisms for single atoms, which should simply hop among lattice sites separated by a distance $a = 2.977$ Å. However, for metal-on-metal epitaxy, small clusters are flat, i.e. they are one-layer-thick islands. For metals on MgO, already dimers and trimers may not stay flat on the surface in their lowest-energy configuration [14]. For example, neutral copper, silver and gold dimers prefer to stay vertical on regular MgO(001) terraces [15, 16], even though the situation can be different on ultrathin films, where gold clusters can be charged [17]. Palladium dimers stay horizontal, but already trimers prefer the vertical configuration [14, 18, 19]. Therefore, we expect that small clusters could present a variety of interesting diffusion mechanisms.

In this paper we review the results on the diffusion of isolated adatoms and small metal clusters on the surface of MgO(001). Due to the difficulty of directly measuring diffusion coefficients and of imaging diffusion processes in experiments, most of the available results have been obtained

 

in the domain of theory and simulations. For this reason, our review will mostly be focused on theoretical results. However, information about the mobility of adatoms and small clusters can be inferred from the effects that such mobility has on quantities that can be more easily measured at the experimental level. When possible, we shall thus compare the predictions that can be inferred from the theoretical results with the experimental observations.

This paper is structured as follows. Section 2 deals with the diffusion of isolated adatoms. Sections 3.1 and 3.2 consider the diffusion of dimers and trimers, while section 3.3 treats the diffusion of tetramers and larger clusters. Section 4 contains the discussion and the conclusions.

## 2. Diffusion of isolated adatoms

### *2.1. Energy barriers for diffusion on the flat surface*

Isolated adatoms on the flat MgO(001) surface diffuse by *hopping* among oxygen sites, which are the most stable for adsorption. The saddle point for diffusion between neighboring oxygen sites is located at the bridge position, which stays in between two magnesium atoms, as shown in figure 1. This has been demonstrated by nudged elastic band (NEB) [20] calculations for several adsorbed metal atoms, including Pd, Ag and Au at least [18, 19, 16]. The energy barrier $E_d$ for this jump process is thus the difference in adsorption energy between oxygen and bridge positions.

Pd/MgO(001) has probably received the greatest attention, so that several calculations of the diffusion barrier for isolated adatoms on the flat terrace are available in the literature. These calculations are all in the framework of density functional theory (DFT), but differ in some aspects, such as in the choice of the exchange–correlation (xc) functional, in either relaxing or not relaxing substrate atoms, in either using a cluster approach for modeling the surface + adatom system or in using supercells. In spite of the different approaches adopted, the values obtained for this barrier are quite similar to each other, thus reinforcing their validity.

Judai *et al* [21] and then Giordano *et al* [22] performed DFT calculations employing the B3LYP xc-functional [23]. They modeled the surface + adatom system by a clusters approach. They also let the substrate neighbors of the adatom relax. From their calculated adsorption energies at oxygen and bridge sites, one can deduce an energy barrier of 0.41 eV for the adatom hopping process.

Vervisch *et al* [7] and Barcaro *et al* [18] adopted a supercell approach, kept the substrate atoms rigid in their bulk-terminated position, with the experimental value of the MgO lattice parameter, and employed the PBE xc-functional [24]. They obtained a barrier of 0.39 eV, thus differing by only 0.02 eV from the value in [21, 22]. Finally, Xu *et al* [19] also used the PBE functional with a supercell, but let the atoms of the top substrate layer relax. They obtained a somewhat lower barrier, of 0.34 eV. This result shows that the relaxation of the substrate does not introduce major changes in diffusion on the flat surface. As we shall see later, substrate relaxation is more important for processes at defects.

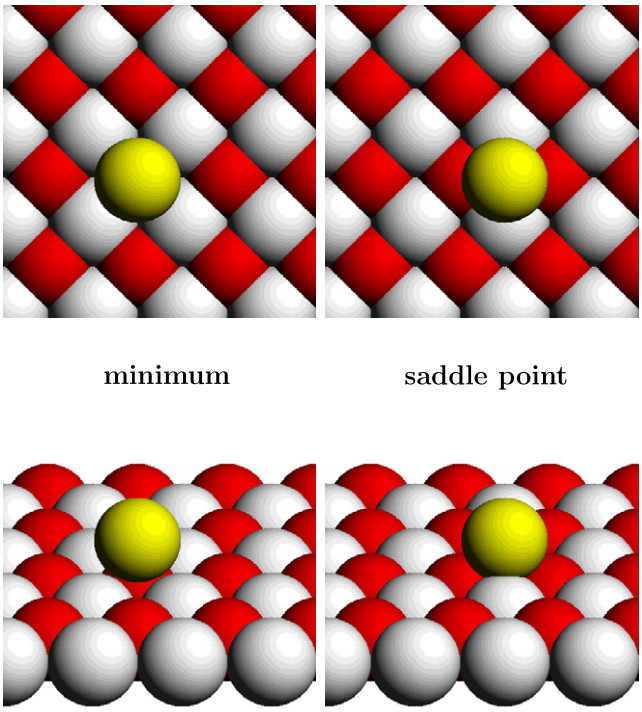


**Figure 1.** Minimum and saddle point positions for hopping diffusion of metal monomers on MgO(001). In the substrate, red (dark gray) and white (light gray) atoms correspond to oxygen and magnesium, respectively. Each position is shown twice, in top and side views.

The diffusion of noble metal atoms has also received some attention. In a pioneering work: Musolino *et al* [15] performed DFT calculations with the PW91 exchange and correlation functional [25] for copper. They obtained a diffusion barrier of 0.36 eV for Cu adatoms on the flat surface. This is a high barrier, practically of the same magnitude as the hopping barrier of Pd, which has, however, a considerably larger adsorption energy than copper. Barcaro and Fortunelli [16] considered the diffusion of Ag and Au within the same computational approach of [18], i.e. with the PBE xc-functional and a rigid substrate. They obtained barriers of 0.10 and 0.22 eV for Ag and Au, respectively. These barriers are much lower than the barrier for Pd atom hopping, as might be expected from the smaller adsorption energy of Ag and Au compared to Pd. In the case of gold it is known that, by changing the xc-functional, calculated properties may vary significantly [26–33]. For this reason, Barcaro and Fortunelli [16] performed calculations within the local-density approximation (LDA) approach for the xc-functional and obtained a somewhat larger barrier of 0.28 eV. On the other hand, Del Vitto *et al* [34] employed the PW91 xc-functional and obtained a barrier of 0.24 eV by relaxing the substrate. This shows again that relaxation of the substrate has no major effect on the diffusion barriers of transition and noble metals on MgO(001).

A detailed study has recently been conducted on the adsorption and diffusion of small Ca clusters on MgO(100) [35]. A Ca monomer was found to diffuse by hopping between nearest-neighbor oxygen sites with a barrier of 0.45 eV, a sizable fraction of its adsorption energy (0.84 eV),

probably due to the loss of charge transfer interactions at the saddle point (the direction of the charge transfer in Ca/MgO is opposite to the Pd/MgO or noble metal/MgO cases).

It should be stressed that here we are considering neutral atoms on thick MgO(100) terraces. Diffusion of charged species can, in principle, present qualitatively different features. In this connection it can be noted that gold atoms have been shown to become negatively charged on properly selected ultrathin ionic films [36, 37]. To the best of our knowledge, the diffusion of the corresponding polaronic species has not been studied at the computational level, while a systematic investigation of cluster formation as a function of temperature has not yet been conducted at the experimental level, even though preliminary results [38] seem to suggest that diffusion coefficients of single atoms might not be too different from those of neutral atoms on thick substrates.

Finally, we recall that diffusion through hopping of adatoms among favorable adsorption sites has been considered on many other oxide surfaces in addition to MgO(100), usually by calculating static energy landscapes whence diffusion energy barriers, see, e.g., [39–41], or occasionally via NEB calculations [42]. Note that the presence of adsorbed species can strongly influence the mobility of metal adatoms, and thus cluster sintering, as shown experimentally for Pd carbonyl-like species on an ultrathin silica film [43].

### 2.2. Long jumps of isolated adatoms

An interesting issue concerning the diffusion of isolated metal adatoms on MgO(001) (and possibly also on other non-polar oxide surfaces) is the possible occurrence of long jumps. In a long jump, the adatom starts from a given adsorption site, travels on the surface and finally thermalizes in a site which is not a nearest neighbor of the site of departure [44, 13, 45, 46]. Long jumps have been observed in the case of metal-on-metal diffusion for several systems [47–51] and also in the diffusion of small and large molecules on metal surfaces [52, 53]. In general, long jumps are favored by a weak dynamic coupling between the substrate and the diffusing adatom, which indeed might be the case of metals on oxides. Let us try to evaluate quantitatively the probability of long jumps for Pd, Ag and Au adatoms.

The MgO(001) substrate is very rigid compared to the above-mentioned metals. For example, the melting temperature of MgO is above 3000 K, while melting temperatures of the adsorbed metals are much lower, from 1235 K (Ag) to 1828 K (Pd). Therefore the typical phonon frequencies of MgO are quite high. In contrast, the frequencies related to the frustrated translations of the adatom on the surface are significantly smaller [19]. This should rule out memory effects in diffusion [54, 13], because the latter are expected to be important when substrate and adatom frequencies are close to each other. This allows the treatment of diffusion within a simple Langevin approach, in which the dynamic coupling between adatom and substrate is described by a simple friction parameter $\eta$, which, together with the temperature, determines also the magnitude of the white noise caused by the substrate [55].

The friction $\eta$ can be decomposed into the sum of a phononic contribution $\eta_{\rm ph}$ and an electronic contribution $\eta_{\rm el}$. The latter is essentially due to the possible creation of electron–hole pairs in the substrate [56]. Due to the insulating nature of the substrate, this process is very unlikely, so that $\eta_{\rm el}$ should be very small, negligible with respect to $\eta_{\rm ph}$. The phononic friction can be easily evaluated by a simple formula which holds for a harmonic substrate, as MgO is expected to be for the temperatures of interest in growth experiments, which are much lower than its melting temperature. The formula for $\eta_{\rm ph}$ follows from an elastic continuum model treatment of the substrate and is [57]

$$\eta_{\rm ph} = \frac{3m}{8\pi\rho}\left(\frac{\omega_{\rm osc}}{c_{\rm T}}\right)^3 \omega_{\rm osc}, \tag{1}$$

where $m$ is the mass of the adatom, $\omega_{\rm osc}$ is the frequency of the frustrated translation of the adatom, $\rho$ is the mass density of the substrate and $c_{\rm T}$ is the transverse sound velocity in the substrate. According to equation (1), $\eta_{\rm ph}$ does not depend on temperature, and this should hold as far as anharmonic effects are negligible. However, within the Langevin model, and assuming that jumps essentially follow straight lines [44] (i.e. assuming that the motions in different directions are uncoupled [58]), the probability of long jumps depends on the dissipation parameter $\Delta$ [59, 44, 60, 61], which can be evaluated as

$$\Delta = \eta_{\rm ph}\frac{2\sqrt{2}a}{\pi k_{\rm B}T}\sqrt{mE_{\rm d}}. \tag{2}$$

The dissipation $\Delta$ is dimensionless and corresponds to the ratio between the energy loss in crossing a single lattice spacing and the thermal energy $k_{\rm B}T$.

Let us discuss the occurrence of long jumps in Pd, Au and Ag on MgO(001).

In the case of Pd, from the model potential of [7] it follows that $\omega_{\rm osc} = 8.76 \times 10^{12}$ rad s$^{-1}$. Taking $c_{\rm T} = 6.62 \times 10^3$ m s$^{-1}$ [62, 63] and $\rho = 3.5761 \times 10^3$ Kg m$^{-3}$, one obtains $\eta_{\rm ph} = 1.25 \times 10^{11}$ s$^{-1}$. This value of the friction is rather low and leads to small dissipation $\Delta$. For example, taking $E_{\rm d} = 0.39$ eV [18], $\Delta = 8.6 \times 10^{-1}$ at $T = 300$ K. Such a value of the dissipation leads to a significant percentage of long jumps [64]. In fact, the model predicts that about 45% of jumps should be long, so that only 55% of the jumps ends in a nearest-neighbor cell. On the other hand, at $T = 200$ K, $\Delta = 1.3$, with a fraction of long jumps of about 40%. This leads to a mean square jump length $L^2 \sim 10a^2$. This might have some consequences on the magnitude of the diffusion coefficient $D$, because the latter is given by

$$D = rL^2 \tag{3}$$

where $r$ is the jump rate in a given direction. The latter assumes the usual Arrhenius form:

$$r = \nu \exp\left(-\frac{E_{\rm d}}{k_{\rm B}T}\right), \tag{4}$$

where $\nu$ is the frequency prefactor, which is often estimated by the transition state theory (TST) [65]. However, TST strongly

overestimates $r$ at low friction, where an energy diffusion regime holds. In the case of Pd, we expect TST to overestimate $r$ by at least a factor of 5.

For Ag, the interaction potential is less corrugated [16, 66], so that $\omega_{\rm osc} = 4.66 \times 10^{12}$ rad s$^{-1}$, which, according to equation (1), leads to a much smaller friction, $\eta_{\rm ph} = 9.77 \times 10^9$ s$^{-1}$, than for Pd. At $T = 300$ K, with $E_{\rm d} = 0.10$ eV [16], $\Delta = 3.4 \times 10^{-2}$, corresponding to a percentage of long jumps of about 90% [64]. At $T = 200$ K, $\Delta = 5.2 \times 10^{-2}$, so that the percentage of long jumps slightly decreases to about 85%. Therefore, the diffusion of single Ag atoms almost completely occurs by long jumps down to very low temperatures, with large percentages of them well below 100 K.

For Au, the interaction potential has intermediate corrugation [16, 66], but the atomic mass is larger, giving $\omega_{\rm osc} = 3.69 \times 10^{12}$ rad s$^{-1}$, which, according to equation (1), leads to an even smaller friction, $\eta_{\rm ph} = 6.99 \times 10^9$ s$^{-1}$, than the friction of Ag. However, mass and corrugation compensate for the lower friction when comparing with Ag. In fact, at $T = 300$ K, with $E_{\rm d} = 0.22$ eV [16], $\Delta = 4.9 \times 10^{-2}$, corresponding to a percentage of long jumps close to 85% [64]. At $T = 200$ K, $\Delta = 7.4 \times 10^{-2}$, so that the percentage of long jumps is nearly 80%. As in Ag, diffusion of single Au is thus expected to be dominated by long jumps down to very low temperatures.

We note that we assumed that all jumps occur in straight lines. This is not true in a multidimensional coupled potential [67, 58], in which there is energy transfer between the $x$, $y$ and $z$ degrees of freedom of the adatom. This energy transfer decreases the percentage of long jumps [58]. According to the model interaction of [7], the coupling between the directions is, however, not strong. Therefore our values of the long jump fraction may be overestimated, but not by a large amount, so that a non-negligible fraction of long jumps should be expected for Pd, Au and Ag on MgO(001).

In the low-friction regime, the jump-length probability distribution of single atoms displays deviation from the exponential decay behavior for short jump distances, while the exponential decay is recovered asymptotically [44]. This rules out the possibility of anomalous diffusion for single adatoms. Anomalous diffusion may occur for larger clusters, which may diffuse by a stick and slip mechanism [68].

Finally we remark that long jumps should be taken into account when calculating the prefactor for adatom diffusion of Pd, Ag and Au. In the case of Pd, the increase of the prefactor due to long jumps is partially compensated by the decrease of the jump rate, so that major effects are not expected. However, for Ag and Au dissipation is considerably weaker and the effect should be more important. In fact, in the limit of $\Delta \ll 1$, the jump rate $r$ decreases as $\Delta$, but $L \propto \Delta^{-2}$, with an increasing effect on the prefactor as follows from equation (3).

### 2.3. Diffusion in the presence of defects

The influence of defects, such as steps and point defects, on diffusion is crucial for understanding the nucleation, growth and phase ordering of adsorbates on crystal surfaces [69–71] in general. In the case of metals on oxides this is even more crucial, since nucleation is often occurring at defects only [72].

The adsorption of Pd, Rh and Ag atoms on steps, edges and corners of MgO has been studied by Judai *et al* [21] and Giordano *et al* [22]. It has been found that oxygen ions are still the preferred adsorption sites for these defects, and that decreasing oxygen coordination usually results in an increase of the metal binding energy to these sites. It can thus be expected that diffusion is inhibited in the presence of these defects, and that they act as trapping and nucleation centers for the growth of metal clusters, as suggested, for example, by the experimental observation of the nucleation of Pd particles along MgO(100) steps [1, 2]. However, it should also be noted that (i) a substantial increase of the binding energy was only observed for Rh atoms adsorbed on steps (about 2 eV instead of about 1 eV on the regular surface) and (ii) real diffusion mechanisms with the corresponding energy barriers and Arrhenius prefactors were not studied explicitly, so that nucleation at such defects might depend on the experimental conditions. A detailed study has instead been conducted for Ca/MgO(100) by Xu and Henkelman [35]. In addition to a rough doubling of the binding energy of Ca atom to steps with respect to flat terraces, it has been found that Ca monomers do not readily diffuse along steps: according to the predicted lowest-energy-barrier mechanism, a Ca atom first leaves the step by crossing a barrier of 1.4 eV to an oxygen site near the step and then hops back to the next site on the step. Steps thus act as strong traps for Ca atoms. Note that, on a different oxide surface, a step-edge (Ehrlich–Schwoebel) barrier has been invoked to rationalize the experimental evidence of increased nucleation at island borders and constant nanoparticle size as a function of coverage [42].

A vast literature exists on the interaction of metal atoms and small clusters with point defects such as the (charged and neutral) oxygen vacancy and the MgO dimer vacancy. It has been shown both theoretically (see, e.g., [73–76] and references therein) and experimentally (see, e.g., [77, 78]) that these defects can act for most metals and cluster sizes as trapping centers, with binding energies for single atoms that can easily surpass 2–3 eV. As far as growth is concerned, the question thus becomes to quantify the detrapping energy barriers corresponding to the dissociation of pieces of clusters adsorbed on the defect (fragmentation). These processes are believed to be the basic mechanisms by which Ostwald ripening and then sintering takes place. A lower bound to fragmentation energy barriers can be derived from the difference between cluster binding energies at defects and on the regular surface. For small clusters, such quantities can be found in several publications for different metal/defect combinations, see, e.g., [79, 4, 80–86, 76, 87, 35]. For Ag clusters on a single oxygen vacancy, due to the peculiar stability of $Ag_2$ on the regular surface, the lowest-energy fragmentation process consists in the detachment of a dimer from a larger metal aggregate. The energy associated with this process was found to grow in an approximately monotonic way with the cluster size from 0.77 eV (the value for $Ag_3$ fragmentation) to 1.6 eV (the value for $Ag_{10}$ fragmentation). A similar behavior was found for Au clusters adsorbed on a single oxygen vacancy, for which fragmentation of a dimer was equally found to be favored (even though with obviously

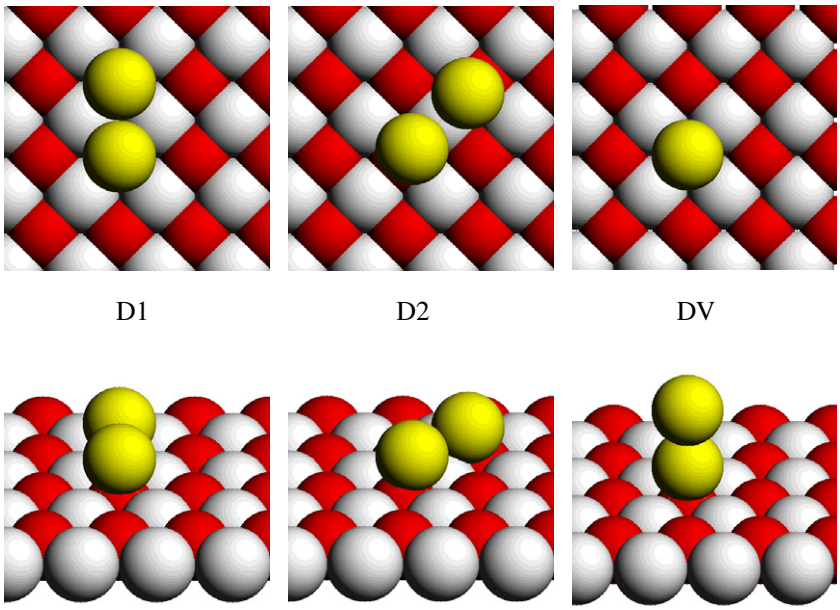


**Figure 2.** Positions D1, D2 and DV (see text) for dimers on MgO(001). In the substrate, red (dark gray) and white (light gray) atoms correspond to oxygen and magnesium, respectively. Each position is shown twice, in top and side views.

different actual values). On the double vacancy, however, the presence of a magic cluster for size $N = 8$ makes that for $N = 9$ the dissociation of a single atom is definitively favored [86], while this is not observed for Au clusters on the same defect due to the lack of magic numbers [87]. In general, dissociation energy differences present a non-monotonic behavior in correspondence with magic clusters and this holds also for binary clusters [85, 76]. The situation is different for the fragmentation of Pd clusters adsorbed on the single vacancy, as a Pd dimer is only marginally stable on the flat terrace or on the oxygen vacancy defect with respect to dissociation into monomers, so that fragmentation of a monomer or of larger clusters, leaving a single Pd atom adsorbed on the defect, can be expected. It should be remarked, however, that the actual barriers can be larger than the static differences between cluster binding energies at defects and on the regular surface, as the dissociating fragment may be forced to pass through unfavorable routes in which contact to the surface (and thus adhesion energy) is lost. To our knowledge, the only example of a full calculation is given in [86] for the '$Ag_9 \rightarrow Ag_8 + Ag$' fragmentation, a special case in which anyway no significant additional barrier was found.

## 3. Diffusion of dimers, trimers and tetramers

### *3.1. Dimers*

A metal dimer on the MgO(100) surface exhibits basically three local minima: one in which the dimer axis is perpendicular to the surface and the basal atom stands on top of an oxygen ion (DV), one in which the dimer axis is parallel to the surface with two metal atoms on nearest-neighbor oxygen atoms (D1) and one in which the dimer axis is parallel to the surface with the metal–metal bond across a magnesium ion (D2), see figure 2. Depending on the relative energetics of these three states one finds different diffusion mechanisms.

For Pd, D1 and D2 are about 1 eV lower in energy than DV and the diffusion takes place via a *rotation* between D1 and D2 involving the motion of one atom at a time, resulting in an intermediate state with an elongated Pd–Pd bond. The weakness of this bond due to intersystem crossing between the $d^{10}$ and $d^9s^1$ atomic configuration of the Pd atom facilitates this mechanism, even though it should be noted that the Pd–Pd distance is contracted with respect to the distance between oxygens and the spin state is a singlet and not a triplet as in the gas-phase species (the metal/surface interaction is often found to quench the cluster spin moment [88]). The barrier for this mechanism is 0.43 eV [19, 83] or 0.39 eV [18] and its Arrhenius prefactor is $2.5 \times 10^{11}$ $s^{-1}$ [19, 83]. Another mechanism involves a concerted *sliding* of the dimer along [110] directions with an energy barrier of 0.60 eV or a dissociation into two monomers with an energy barrier of 0.80 eV [19, 83].

For noble metal atoms, we found an opposite situation with the energy ordering: DV < D1 < D2, due to the 'metal-on-top' stabilization mechanism [5]. For Cu, the energy difference between the DV and D1 configurations, $\Delta E$ (DV–D1), is 0.04 eV [15] or 0.28 eV [5] (this is one of the rare cases in which we find a significant discrepancy between calculations using similar xc-functionals but different computational methods). Accordingly, the $Cu_2$ dimer can diffuse, either remaining in the DV configuration and hopping between nearest-neighbor oxygen sites with a barrier of 0.56 eV, or via a *leapfrog* [89] mechanism in which DV rotates into D1 that in turn rotates back into a DV on a nearest-neighbor site with a barrier of 0.17 eV [15]. Even taking into account discrepancies in the calculation of $\Delta E$ (DV–D1), the final energy barrier for this mechanism should not be larger than 0.4 eV, and thus comparable with that of the monomer. For Ag, $\Delta E$ (DV–D1) is 0.22 eV and $Ag_2$ can diffuse either via dimer hopping with a barrier of 0.25 eV or via a leapfrog

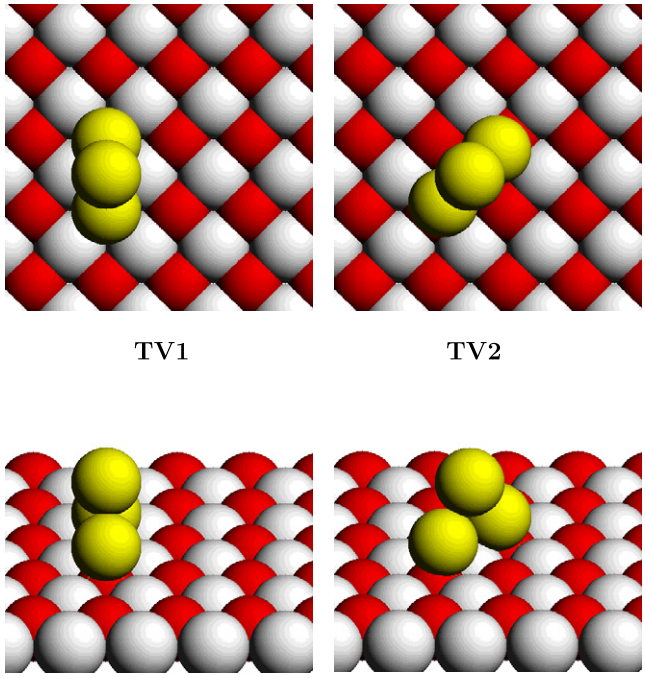


**Figure 3.** Positions TV1 and TV2 (see text) for vertical trimers on MgO(001). In the substrate, red (dark gray) and white (light gray) atoms correspond to oxygen and magnesium, respectively. Each position is shown twice, in top and side views.

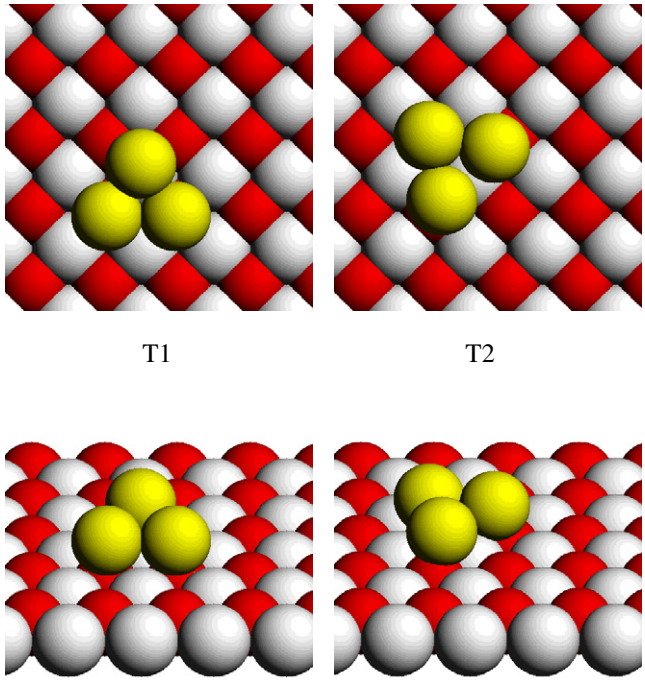


**Figure 4.** Positions T1 and T2 (see text) for flat trimers on MgO(001). In the substrate, red (dark gray) and white (light gray) atoms correspond to oxygen and magnesium, respectively. Each position is shown twice, in top and side views.

mechanism with a barrier of 0.22 eV, practically coincident with $\Delta E$ (DV–D1) [16]. Analogously for Au $\Delta E$ (DV–D1) is 0.87 eV and $Au_2$ can diffuse either via dimer hopping with a barrier of 0.62 eV or via a leapfrog mechanism with a barrier that has not been calculated explicitly but must be larger than 0.87 eV, i.e. the $\Delta E$ (DV–D1) energy difference [16]. We thus find that in the Ag and Au cases the dimer, although not epitaxial, has diffusion energy barriers appreciably larger than the monomer.

A still different case is that of an alkali-earth element such as Ca. In this case, the $Ca_2$ bond is really weak. The maximum adsorption energy (0.88 eV/atom) is achieved in the D2 configuration and is only marginally stable than the sum of two Ca monomers (0.84 eV), while the D1 configuration has an adsorption energy of 0.78 eV/atom and is thus metastable. $Ca_2$ in the D2 configuration can either diffuse via rotation to D1 with a barrier of 0.50 eV or via dissociation into monomers with a barrier of 0.30 eV, and thus with a mobility comparable with that of a monomer.

### *3.2. Trimers*

A metal trimer on the MgO(100) surface exhibits at least five local minima: a linear one with a metal atom on top of an O ion and the other two atoms along a [110] direction (L); two vertical ones (see figure 3), in which the trimer is adsorbed in an upright position and the cluster plane can be either oriented along a [110] direction with the two basal metal atoms on top of nearest-neighbor oxygen ions (TV1) or oriented along a [100] direction with the two basal metal atoms pointing towards two next-nearest-neighbor oxygen ions and a magnesium atom beneath the center of mass of the cluster (TV2); and finally two flat ones, in which the cluster plane is lying on the surface and two metal atoms can either be adsorbed on top of nearest-neighbor oxygen ions while the third one points towards a magnesium ion (T1) or can be across a magnesium ion while the third one sits on an oxygen ion (T2), see figure 4. The diffusion mechanisms again depend on the relative energetics of these five configurations.

The metal-on-top effect stabilizes upright configurations with respect to planar ones for both Pd and noble metal trimers. The lowest-energy minimum is TV1, with TV2 higher in energy by 0.19–0.27 eV for Pd [18, 19, 83], 0.15–0.25 eV for Cu [15, 5], 0.01–0.06 eV for Ag [5, 16] and 0.12–0.14 eV for Au [5, 16]. The T1 planar configuration lies higher in energy: the TV1–T1 energy difference is 0.28 eV for Pd [19, 83], 0.50–0.56 eV for Cu [15, 16] and 0.24 eV for Ag, while it is not even a local minima for Au [5] (T2 is even higher in energy for Pd: 0.44 eV [19, 83]). Cu is the only metal for which the linear configuration is competitive with the planar ones, being 0.33 eV higher than T1 [15]. The upright character of the lowest-energy structures, added to the fluxional character of the trimer for these metals, i.e. the possibility of stretching metal–metal bonds due to their anti-bonding components, makes that trimer diffusion on MgO(100) is facile.

In particular, for Ag and Au the metal-on-top effect stabilizes the upright configurations so much that TV1–TV2 rotation or trimer *walking* represents by far the lowest-energy mechanism, with barriers of 0.12 eV for Ag and 0.19 eV for Au [16], i.e. fully comparable to those of the monomers. For Cu, the barrier for trimer walking was not calculated in [15], but a different *concertina* mechanism was found in which the

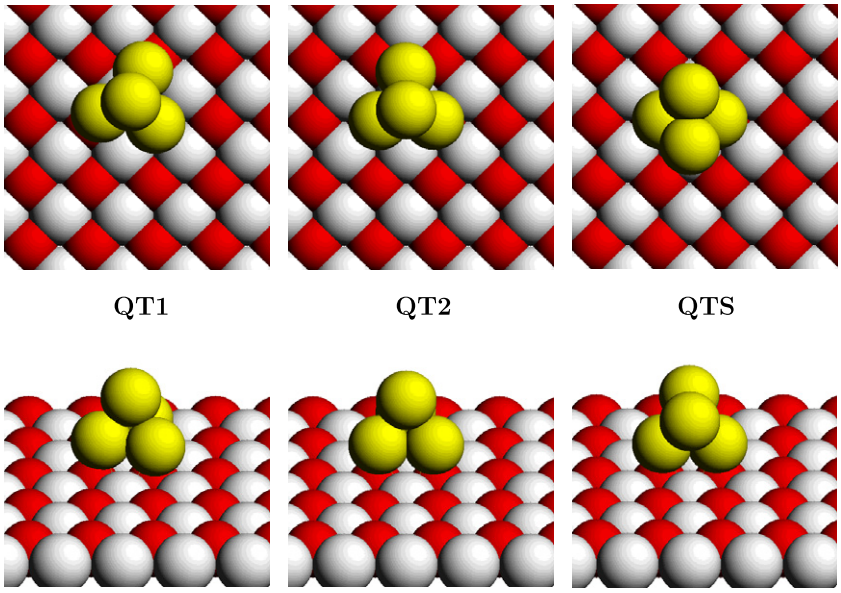


**Figure 5.** Positions QT1, QT2 and QTS (the latter is a saddle point configuration, see text) for tetrahedral tetramers on MgO(001). The diffusion of Pd tetrahedra takes place through the sequence QT1 → QT2 → QTS → QT2 → QT1 and so on. In the substrate, red (dark gray) and white (light gray) atoms correspond to oxygen and magnesium, respectively. Each position is shown twice, in top and side views.

top atom of TV1 moves down to a surface oxygen to form an L configuration and then the Cu atom at the other end of the line moves up to form a TV1 triangle displaced by one lattice unit. The barrier for this process was found to be 0.50 eV. For Pd, instead, the metal-on-top effect is less important and the situation is more varied. TV1–TV2 rotation still represents a low-energy mechanism with a barrier of 0.30 [18] or 0.48 and a prefactor of $5.4 \times 10^{10}$ $s^{-1}$ [83] eV. However, there is a *flipping* mechanism in which the top atom of TV1 flips down to the surface forming T1, from which a different atom can lift onto the other two, forming TV1 in a different location. According to [19, 83], the barrier for this process is 0.50 eV, but its prefactor is much larger than the walking mechanism: $1.1 \times 10^{13}$ $s^{-1}$ so that it is expected to dominate at high (and even low) temperatures. Flat trimers can also diffuse but with high barriers (at least 1–1.4 eV) [83].

For Ca, the lowest-energy trimer configurations are flat, but their adsorption energy is smaller than three times the monomer adsorption energies, so that they represent metastable states [35].

### *3.3. Tetramers and larger clusters*

Four local minima are mostly involved in the diffusion mechanisms of metal tetramers studied in the previous literature: two tetrahedral arrangements lying on the surface with three contact atoms in which the basal atoms are either positioned as in the T2 configuration (QT1) or as in the T1 configuration (QT2) (see figure 5), and two vertical arrangements, in which the cluster has a rhomboidal shape, interacts with the surface through two basal atoms and the cluster plane is either oriented along the [100] direction (QV1) or the [110] direction (QV2), see figure 6.

For Pd, the tetrahedral structures QT1 and QT2 (with QT1 being the absolute minimum) are lower in energy than flat configurations by more than 1 eV [83] (and are also lower in energy than vertical configurations). The latter thus do not have a role in tetramer diffusion, which occurs via a *rolling* mechanism involving tetrahedral configurations only. QT1, in fact, first transforms into QT2 by a small-angle rotation around a vertical axis, after which QT2 rotates around a horizontal axis passing through the two Pd atoms positioned on top of the oxygens (this is the saddle point configuration QTS in figure 5) ending up in a different QT2 configuration displaced by one lattice spacing with respect to the initial one [18, 19, 83]. From this position, another small-angle rotation can produce a new QT1 configuration. The barrier for this sequence of moves is 0.38 eV [18] or 0.42 eV and a prefactor of $1.3 \times 10^{14}$ $s^{-1}$ [19, 83]. An identical mechanism is effective for $Ca_4$ diffusion on MgO(100), in which case the energy barrier is only 0.12 eV, an absolute minimum among the barriers involving small Ca clusters [35]. QT1 can also diffuse by sliding with a global barrier of 0.45 eV [18] or 0.51 eV and a prefactor of $1.0 \times 10^{13}$ $s^{-1}$ [19, 83], but this mechanism is not favored with respect to tetramer rolling.

A weaker metal/surface interaction favors vertical arrangements (QV1 and QV2) with respect to compact ones (QT1 and QT2) for noble metal clusters, thus giving rise to quite different diffusion mechanisms. Actual values for energy barriers and prefactors were not calculated for $Cu_4$ on MgO in [15], but snapshots from Carr–Parrinello simulations were reported, showing planar arrangements not heavily linked to the substrate, and it was pointed out that the observation of diffusion at low temperature (100 K) and in short runs (a few ps) implied that diffusion barriers are quite small for this system, of the same order as those of the dimer and thus smaller than the barriers for the monomer and trimer. In this system metal bonding prevails and $Cu_4$ diffuses via *twisting* mechanisms in which an adatom first detaches from the

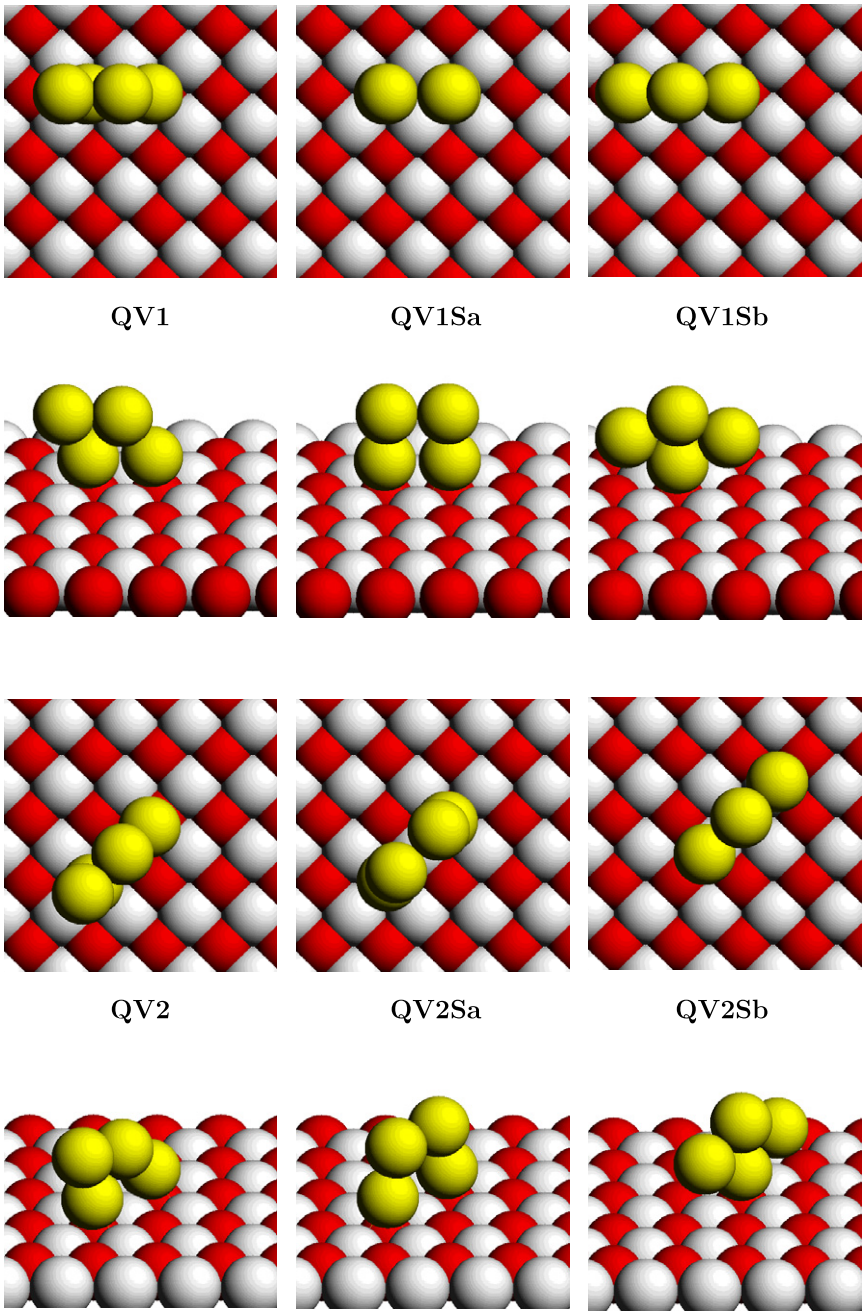


**Figure 6.** Positions QV1, QV1Sa, QV1Sb, QV2, QV2Sa and QV2Sb (see text) for vertical tetramers on MgO(001). QV1 and QV2 are minimum positions, whereas QV1Sa, QV1Sb, QV2Sa and QV2Sb are saddle point positions. In the substrate, red (dark gray) and white (light gray) atoms correspond to oxygen and magnesium, respectively. Each position is shown twice, in top and side views.

surface, rotates around a 'pivot' adatom which remains bonded to the surface, and finally readsorbs in a different position on the surface. A more detailed analysis was conducted for Ag and Au in [16]. It can be noted that for both metals the tetramer is a closed-shell system with a reduced fluxional character with respect to the trimer. However, silver and gold presents subtle differences, despite their similarities, in the energetics of their local minima and thus of their diffusion behavior. To begin with, QV2 is found as the global minimum for Au, with QV1 at a slightly higher energy ($\Delta E$ of 0.15 eV), whereas QV1 is the global minimum for Ag, with QV2 at a slightly higher energy ($\Delta E = 0.04$ eV). Moreover, the diffusion of Ag and Au tetramers can take place through a variety of mechanisms, which are different in the two cases. One possibility is represented by a movement of tetramer walking between configurations QV1 and QV2, a movement analogous to trimer walking. The difference with respect to the trimer is that the rotation of 45° can take place either around the vertex at higher coordination or around the vertex at lower coordination: the two movements have different barriers as it is energetically less costly to move the basal atom with lower coordination with respect to the basal atom with higher coordination, because the

former loses less metal-on-top or metal-bonding stabilization energy. In the case of gold, the values of the two energy barriers are 0.38 and 0.60 eV, respectively; in the case of silver 0.10 and 0.21 eV. Since a tetramer needs both movements for real diffusion (a single rotation does not allow the cluster to leave an area of four first-neighbor oxygen sites) the real value of the barrier is thus 0.60 eV for gold and 0.21 eV for silver. Therefore, despite the similarities between the walking mechanisms in the trimers and tetramers, the need to move an atom with higher coordination makes the diffusion energy barrier for the tetramer higher than that for the trimer. However, while in the case of silver the tetramer walking mechanism corresponds to the diffusion mechanism with the lowest barrier, in the case of gold other processes have a lower activation energy. The QV2 configuration, in fact, can move along the [100] direction to another QV2 configuration through a first *rocking* mechanism, i.e. passing through the saddle point QV2Sa—barrier of 0.39 eV—and then through a *rolling* mechanism, i.e. passing through the saddle point given by the configuration QV2Sb—barrier of 0.44 eV. This rolling movement (to be distinguished from the qualitatively different movement of the tetrahedron) consists of revolving the cluster around the most coordinated atom in direct contact with the surface. The combination of these two movements determines a diffusion of the tetramer along the [100] direction; the barrier is given by the higher value between the two values found: 0.44 eV. Still another possibility is that QV2 first rotates into QV1 through the first step of the walking mechanism, and that QV1 then diffuses through successive rocking/rolling movements along the [110] direction in a way completely analogous to the diffusion of QV2 along the [100] direction. A QV1 configuration thus rocks into another QV1 configuration through the saddle point QV1Sa—barrier of 0.27 eV—and rolls into another QV1 configuration through the saddle point QV1Sb—barrier of 0.25 eV. The barrier for this mechanism is given by the sum of the energy difference between QV2 and QV1—0.15 eV—and the higher of the two rocking/rolling barriers—0.27 eV—for a total of 0.42 eV. The rocking/rolling processes in the two directions are thus energetically equivalent and both very favorable with respect to the walking mechanism. These rocking/rolling movements are not competitive in the case of silver because they pass through the saddle points QV1Sa and QV2Sa which present a remarkable distortion of the metal bonding, a distortion not compensated by an enhanced direct adhesion to the surface nor by the metal-on-top effect.

To conclude this section, we recall that the mobility of large metal clusters on MgO(100) is a fascinating subject which, however, has not yet been investigated at the computational level. Experimental observations as well as theoretical simulations on different (especially non-epitaxial) systems indicate that large aggregates can be mobile under given conditions [90–93]. Experiments seem to suggest that similar phenomena can occur also on oxides, see, e.g., [94, 95] (and references therein), where surface diffusion rather than static coalescence has been invoked to rationalize observed power-law behavior of the growth of Pt nanoclusters on MgO(100) and Au nanoclusters on $TiO_2(110)$. All this is left for future work.

## 4. Discussion and conclusions

From the analysis of the existing literature on the subject, it can be concluded that the diffusion of metal adatoms and small clusters on the (001) surface of magnesium oxide can occur via a variety of processes. Apart from simple hopping between favorable adsorption sites, rotation, sliding, leapfrog, walking, concertina, flipping, twisting, rolling and rocking mechanisms have been shown to take place, depending on the type of metal (i.e. the features of its interaction with the surface) and the size of the cluster. It is difficult to predict *a priori* which mechanism will be dominant in each specific case, as the actual values of the energy barriers and prefactors strongly depend on fine details of the interplay between metal–metal and metal–surface interaction. As far as the latter is concerned, charge transfer effects from/to the surface, relative components of covalent bond versus electrostatic polarization of the electronic cloud and metal-on-top effects can all play a role.

A general statement can, however, be made in all the considered cases. Small clusters at least up to the tetramer have been found to exhibit diffusion coefficients comparable with, and in some cases even appreciably larger than, that of the monomer. Since aggregation of deposited atoms into small clusters as well as detachment of small fragments from a cluster trapped on a defect are common phenomena, diffusion of small clusters is extremely significant in the effect of growth understanding and simulation, and should not be ignored, as we discuss below in connection with the interpretation of Pd growth experiments.

Once diffusion coefficients and detrapping probabilities as a function of the cluster size together with the topography of the surface adsorption and nucleation sites are given, the kinetics of cluster nucleation, growth and sintering can then be simulated [96, 18, 19, 83, 97–101, 97, 102–105] and the results compared to experiments.

An experiment that has stimulated much theoretical work was performed by Haas *et al* [72], who epitaxially deposited Pd adatoms on MgO(001) in a wide range of temperatures, from 200 to 800 K, and measured the temperature-dependent island density $n_I$. They found that $n_I$ is constant from 200 to about 600 K, and drops suddenly down above this temperature.

The constant island density was an indication of nucleation at defects down to low temperatures, with a negligible proportion of terrace nucleation. From this result, Haas *et al* deduced that there should be a substantial mobility of palladium down to 200 K. They attributed the mobility to palladium monomers diffusing and, assuming a prefactor $\nu = 3 \times 10^{12}$ s$^{-1}$, estimated $E_d < 0.3$ eV. The assumed prefactor for the jump frequency was larger than the one calculated by Xu *et al* [19], who obtained $\nu = 7.4 \times 10^{11}$ s$^{-1}$. However, in calculating the diffusion coefficient, that difference could be compensated by the occurrence of long jumps. The experimental estimate of $E_d$ was at variance with all DFT calculations, which give 0.34 eV $\leqslant E_d \leqslant$ 0.41 eV [7, 21, 22, 19, 18]. The discrepancy between the experimental estimate and the calculations was solved by noting that small clusters, up to the tetramer, also strongly contribute to the mobility of palladium down to

200 K [19, 18], so that trimers or tetramers may be even more mobile than monomers. Therefore, in determining whether nucleation occurs either on terrace sites or at defects, the mobility of monomers and of small clusters must be taken into account [18].

Nucleation at defects imply that defects should act as traps for palladium monomers and clusters. Haas *et al* deduced a high trapping energy $E_t \geqslant 1.2$ eV for monomers, so that the drop of the island density at high temperatures was attributed to the breaking of clusters at traps, followed by incomplete condensation, and not to the detachment of monomers from the traps. This picture is consistent with the theoretical results mentioned in section 2.3, which give large values for $E_t$, even in the range of 2–3 eV, but much lower fragmentation energies for at least some small clusters at defects. Finally, rate-equation calculations [105], based on DFT detrapping and fragmentation energies, explained the drop in island density at high temperatures in terms of nucleation at $F_s^+$ and divacancy centers, obtaining a very good agreement with the experimental results.

When comparing with experiments, a warning should be kept in mind. Diffusion of metal adatoms and clusters on MgO(001) is a low-friction phenomenon, and this renders the theoretical evaluation of the frequency prefactors $r$ (equation (4)) and of the mean square jump lengths $L^2$ more difficult. These quantities have an important role in determining diffusion coefficients, as follows from equation (3), and therefore nucleation rates and sites.

In fact, the discussion in section 2 has shown that long jumps of isolated adatoms can be numerous (or even dominant) with respect to nearest-neighbor ones. This could be expected to reinforce the role of monomer, rather than cluster, diffusion, but it should be taken into account that long jumps may occur equally well for small clusters. To our knowledge, however, such an analysis has not been conducted until now. Arrhenius prefactors and their influence on diffusion are also difficult to assess. At low friction, transition state theory can strongly overestimate the rates. Moreover, anharmonic effects may come into play when temperature is raised, so that the harmonic approximation to TST may become questionable.

A further remark concerns the strongly non-monotonic behavior of the diffusion energy barriers with cluster size: see, e.g., the Ag and Au cases with the odd/even alternation of barrier values, or the Ca/MgO case, in which $Ca_4$ diffuses with an energy barrier that is 3.7 times smaller than that of the isolated adatom. Collective movements can thus make diffusion more facile rather than hindering it.

Naturally, the conclusion about the importance of small cluster diffusion can be influenced by the fact that we are considering here the extreme non-scalable regime, i.e. the size range in which 'each atom counts' and in which most of the lowest-energy structures are non-epitaxial. It could be expected that in passing to larger, epitaxial systems cluster mobility should eventually be quenched. It can be noted, however, that in dynamic conditions, such as those typical during growth, metal clusters cannot be considered as static objects with a fixed (frozen) shape. Rather, incorporation of incoming adatoms is likely to pass via defective local minima, which will eventually rearrange to more stable configurations through dynamic processes, possibly involving movement of the center of mass of the cluster. Moreover, the heat evolved in the 'cluster + adatom' reaction will also take some time before being dissipated and in this period provide energy to facilitate overcoming activation barriers. These and other possible effects seem to be necessary to rationalize experimental observations concerning the diffusion of large clusters under typical growth conditions [94, 95].

To conclude, metal diffusion on oxide surfaces is a subject of apparent importance in the general field of supported nanoparticles. Despite recent progress, several unanswered questions still exist in this subject, ranging from the role of long jumps to diffusion mechanisms of charged species or in non-equilibrium conditions, opening the way for future investigations to stimulate, which is one of the aims of the present review.

## References


[1] Henry C R 1998 *Surf. Sci. Rep.* **31** 235
[2] Henry C R 2005 *Prog. Surf. Sci.* **80** 92
[3] Li C, Wu R, Freeman A J and Fu C L 1993 *Phys. Rev.* B **48** 8317
[4] Giordano L, Di Valentin C, Goniakowski J and Pacchioni G 2004 *Phys. Rev. Lett.* **92** 096105
[5] Barcaro G and Fortunelli A 2005 *J. Chem. Theory Comput.* **1** 972
[6] Musolino V, Dal Corso A and Selloni A 1999 *Phys. Rev. Lett.* **83** 2761
[7] Vervisch W, Mottet C and Goniakowski J 2002 *Phys. Rev.* B **65** 245411
[8] Barcaro G, Fortunelli A, Nita F, Rossi G and Ferrando R 2007 *Phys. Rev. Lett.* **98** 156101
[9] Ferrando R, Rossi G, Nita F, Barcaro G and Fortunelli A 2008 *ACS Nano* **2** 1849
[10] Rossi G, Mottet C, Nita F and Ferrando R 2006 *J. Phys. Chem.* B **110** 7436
[11] Olander J, Lazzari R, Jupille J, Mangili B, Goniakowski J and Renaud G 2007 *Phys. Rev.* B **76** 075409
[12] Tian W, Sun H P, Pan X Q, Yu J H, Yeadon M, Boothroyd C B, Feng Y P, Lukaszew R A and Clarke R 2005 *Appl. Phys. Lett.* **86** 131915
[13] Ala-Nissila T, Ferrando R and Ying S C 2002 *Adv. Phys.* **51** 949
[14] Yudanov I, Pacchioni G, Neyman K and Rösch N 1999 *Surf. Sci.* **426** 123
[15] Musolino V, Selloni A and Car R 1999 *Phys. Rev. Lett.* **83** 3242
[16] Barcaro G and Fortunelli A 2007 *New J. Phys.* **9** 22
[17] Simic-Milosevic V, Heyde M, Nilius N, König T, Rust H-P, Sterrer M, Risse T, Freund H-J, Giordano L and Pacchioni G 2008 *J. Am. Chem. Soc.* **130** 7814
[18] Barcaro G, Fortunelli A, Nita F and Ferrando R 2005 *Phys. Rev. Lett.* **95** 246103
[19] Xu L, Henkelman G, Campbell C T and Jönsson H 2005 *Phys. Rev. Lett.* **95** 146103
[20] Henkelman G, Uberuaga B P and Jonsson H 2000 *J. Chem. Phys.* **113** 9901
[21] Judai K, Abbet S, Wörz A S, Heiz U, Giordano L and Pacchioni G 2003 *J. Phys. Chem.* B **107** 9377
[22] Giordano L, Del Vitto A, Pacchioni G and Ferrari A M 2004 *Surf. Sci.* **540** 63
[23] Becke A D 1996 *Phys. Rev.* A **38** 3865

[24] Perdew J P, Burke K and Ernzerhof M 1996 *Phys. Rev. Lett.* **77** 3865
[25] Perdew J P, Chevary J A, Vosko S H, Jackson K A, Pederson M R, Singh D J and Fiolhais C 1992 *Phys. Rev.* B **46** 6671
[26] Bonačič-Koutecky V, Burda J, Mitrič R, Ge M, Zampella G and Fantucci P 2002 *J. Chem. Phys.* **117** 3120
[27] Fernandez E M, Soler J M, Garzón I L and Balbas L C 2004 *Phys. Rev.* B **70** 165403
[28] Soulé de Bas B, Ford M J and Cortie M B 2004 *J. Mol. Struct. (Theochem)* **686** 193
[29] Pyykkö P and Runeberg N 2004 *Angew. Chem. Int. Edn* **41** 2174
[30] Pyykkö P 2005 *Inorg. Chim. Acta* **358** 4113
[31] Remacle F and Kryachko E S 2004 *Advances in Quantum Chemistry* (Amsterdam: Elsevier)
[32] Remacle F and Kryachko E S 2005 *J. Chem. Phys.* **122** 044304
[33] Aprà E, Ferrando R and Fortunelli A 2006 *Phys. Rev.* B **73** 205414
[34] Del Vitto A, Pacchioni G, Delbecq F and Sautet P 2005 *J. Phys. Chem.* B **109** 8040
[35] Xu L and Henkelman G 2008 *Phys. Rev.* B **77** 205404
[36] Repp J, Meyer G, Olsson F E and Persson M 2004 *Science* **305** 493
[37] Pacchioni G, Giordano L and Baistrocchi M 2005 *Phys. Rev. Lett.* **94** 226104
[38] Heyde M, Rust H-P, Sterrer M, Risse T and Freund H-J 2007 *Phys. Rev. Lett.* **98** 206103
[39] Corral Valero M, Raybaud P and Sautet P 2006 *J. Phys. Chem.* B **110** 1759
[40] Katsiev K, Batzill M, Diebold U, Urban A and Meyer B 2007 *Phys. Rev. Lett.* **98** 186102
[41] Matthey D, Wang J G, Wendt S, Matthiesen J, Schaub R, Laegsgaard E, Hammer B and Besenbacher F 2007 *Science* **315** 1692
[42] Sedona F, Sambi M, Artiglia L, Rizzi G A, Vittadini A, Fortunelli A and Granozzi G 2008 *J. Phys. Chem.* C **112** 3187
[43] Lu J-L, Kaya S, Weissenrieder J, Gao H-J, Shaikhutdinov S and Freund H J 2006 *Surf. Sci.* **600** L153
[44] Ferrando R, Spadacini R and Tommei G E 1993 *Phys. Rev.* E **48** 2437
[45] Miret-Artes S and Pollak E 2005 *J. Phys.: Condens. Matter* **17** S4133
[46] Antczak G and Ehrlich G 2007 *Surf. Sci. Rep.* **62** 39
[47] Frenken J W M, Hinch B J, Toennies J P and Wöll C 1990 *Phys. Rev.* B **41** 938
[48] Ellis J and Toennies J P 1993 *Phys. Rev. Lett.* **70** 2118
[49] Cowell-Senft D and Ehrlich G 1995 *Phys. Rev. Lett.* **74** 294
[50] Linderoth T R, Horch S, Laegsgaard E, Stensgaard I and Besenbacher F 1997 *Phys. Rev. Lett.* **78** 4978
[51] Antczak G and Ehrlich G 2004 *Phys. Rev. Lett.* **92** 166105
[52] Alexandrowicz G, Jardine A P, Fouquet P, Dworski S, Allison W and Ellis J 2004 *Phys. Rev. Lett.* **93** 156103
[53] Schunack M, Linderoth T R, Rosei F, Laegsgaard E, Stensgaard I and Besenbacher F 2002 *Phys. Rev. Lett.* **88** 156102
[54] Cucchetti A and Ying S C 1996 *Phys. Rev.* B **54** 3300
[55] Risken H 1989 *The Fokker–Planck Equation* (Berlin: Springer)
[56] Persson B N J 1998 *Sliding Friction—Physical Principles and Applications* (Berlin: Springer)
[57] Persson B N J and Rydberg R 1985 *Phys. Rev.* B **32** 3586
[58] Ferrando R, Spadacini R, Tommei G E and Caratti G 1996 *Phys. Rev.* E **54** 4708
[59] Melnikov V I 1991 *Phys. Rep.* **209** 1
[60] Ferrando R, Spadacini R, Tommei G E and Caratti G 1994 *Surf. Sci.* **311** 411
[61] Ferrando R, Spadacini R, Tommei G E and Caratti G 1993 *Physica* A **195** 506
[62] Singh R K and Upadhyaya K S 1972 *Phys. Rev.* B **6** 1588
[63] Sangster M J L, Peckham G and Saunderson D H 1970 *J. Phys. C: Solid State Phys.* **3** 1026
[64] Ferrando R, Spadacini R and Tommei G E 1995 *Phys. Rev.* E **51** 126
[65] Hanggi P, Talkner P and Borkovec M 1990 *Rev. Mod. Phys.* **62** 251
[66] Goniakowski J, Jelea A, Mottet C, Barcaro G, Fortunelli A, Kuntová Z, Nita F, Levi A C, Rossi G and Ferrando R 2009 *J. Chem. Phys.* submitted
[67] Chen L Y, Baldan M R and Ying S C 1996 *Phys. Rev.* B **54** 8856
[68] Luetdtke W D and Landman U 1999 *Phys. Rev. Lett.* **82** 3835
[69] Masin M, Vattulainen I, Ala-Nissila T and Chvoj Z 2003 *Surf. Sci.* **544** L703
[70] Chvoj Z, Masin M and Ala-Nissila T 2006 *J. Stat. Mech.* P10003
[71] Masin M, Vattulainen I, Ala-Nissila T and Chvoj Z 2007 *J. Chem. Phys.* **126** 114705
[72] Haas G, Menck A, Brune H, Barth J V, Venables J A and Kern K 2000 *Phys. Rev.* B **61** 11105
[73] Neyman K M, Inntam C, Matveev A V, Nasluzov V A and Rösch N 2005 *J. Am. Chem. Soc.* **127** 11652
[74] Barcaro G, Causà M and Fortunelli A 2007 *Theor. Chem. Acc.* **118** 807
[75] Florez E, Mondragòn F, Fuentealba P and Illas F 2001 *Phys. Rev.* B **63** 155408
[76] Barcaro G and Fortunelli A 2008 *Faraday Discuss.* **128** 37
[77] Sterrer M, Fischbach E, Risse T and Freund H J 2005 *Phys. Rev. Lett.* **94** 186101
[78] Barth C and Henry C R 2003 *Phys. Rev. Lett.* **91** 196102
[79] Bogicevic A and Jennison D R 2002 *Surf. Sci.* **515** L481
[80] Inntam C, Moskaleva L V, Neyman K M, Nasluzov V A and Rösch N 2006 *Appl. Phys.* A **82** 181
[81] Neyman K M, Inntam C, Moskaleva L V and Rösch N 2006 *Chem. Eur. J.* **12** 277
[82] Barcaro G and Fortunelli A 2006 *J. Phys. Chem.* B **110** 21021
[83] Xu L, Henkelman G, Campbell C T and Jönsson H 2006 *Surf. Sci.* **600** 1351
[84] Barcaro G, Aprà E and Fortunelli A 2007 *Chem. Eur. J.* **13** 6408
[85] Barcaro G and Fortunelli A 2007 *J. Phys. Chem.* C **111** 11384
[86] Barcaro G and Fortunelli A 2007 *Phys. Rev.* B **76** 165412
[87] Barcaro G and Fortunelli A 2008 *Chem. Phys. Lett.* **457** 143
[88] Markovits A, Paniagua J C, Lopez N, Minot C and Illas F 2003 *Phys. Rev.* B **67** 115417
[89] Montalenti F and Ferrando R 1999 *Phys. Rev. Lett.* **82** 1498
[90] Bardotti L, Jensen P, Hoareau A, Treilleux M and Cabaud B 1995 *Phys. Rev. Lett.* **74** 4694
[91] Deltour P, Barrat J-L and Jensen P 1997 *Phys. Rev. Lett.* **78** 4597
[92] Jensen P 1999 *Rev. Mod. Phys.* **71** 1695
[93] Carrey J, Maurice J-L, Petroff F and Vaurès A 2001 *Phys. Rev. Lett.* **86** 4600
[94] Olander J, Lazzari R, Jupille J, Mangili B, Goniakowski J and Renaud G 2007 *Phys. Rev.* B **76** 075409
[95] Lazzari R, Renaud G, Jupille J and Leroy F 2007 *Phys. Rev.* B **76** 125412
[96] Campbell C T, Parker S C and Starr D E 2002 *Science* **298** 811
[97] Xu L, Campbell C T, Jönsson H and Henkelman G 2007 *Surf. Sci.* **601** 3133
[98] Parker S C and Campbell C T 2007 *Phys. Rev.* B **75** 035430
[99] Parker S C and Campbell C T 2007 *Top. Catal.* **44** 3
[100] Chen P, Wang T Y and Luo M F 2007 *J. Chem. Phys.* **127** 144714

[101] Vasco E and Sacedòn J L 2007 *Phys. Rev. Lett.* **98** 036104
[102] Zhdanov V P 2008 *Surf. Rev. Lett.* **15** 217
[103] Zeng Q H, Wong K, Jiang X C and Yu A B 2008 *Appl. Phys. Lett.* **92** 103109
[104] Zhu J, Farmer J A, Ruzycki N, Xu L, Campbell C T and Henkelman G 2008 *J. Am. Chem. Soc.* **130** 2314
[105] Venables J A, Giordano L and Harding J H 2006 *J. Phys.: Condens. Matter* **18** S411